Supporting Information

Arranz et al. 10.1073/pnas.1119038109

SI Materials and Methods

Cell Culture. For isolation of alveolar macrophages, bronchoalveolar lavage fluid was obtained through intratracheal instillation of PBS. Red blood cells were lysed using ammonium chloride lysis buffer (Sigma-Aldrich). More than 90% of the cells isolated this way were macrophages as was confirmed by CD11c and F4/80 expression using flow cytometry. Isolated cells were used for RNA extraction, and Arg1 expression was analyzed by real-time RT-PCR as described below.

Silencing Experiments. Raw264.7 macrophages were infected with a lentivirus (pLKO.1-puro) expressing a short hairpin (sh) of Akt1 or an sh of Akt2, prepared in HEK293T cells as described previously (1). For controls, an empty vector was used. Infection was quantified using a control lentivirus expressing GFP, which confirmed infection of ∼80% of the cells. Cells were cultured for 72 h following infection. Effective silencing was evaluated by Western blot analysis, and the sh constructs with better efficiency were selected for further experiments: sh1-2 for Akt1 and sh1-3 for Akt2 (Fig. S4).

ELISA. Cytokine concentration in serum and cell culture supernatants was determined by ELISA at the indicated time points using ELISA kits (R&D Systems), according to the manufacturer's instructions. Serum IL-4 was measured using an in vivo capture approach in which IL-4 capture antibody was injected i.v. in mice and sera were collected 24 h later (BD Biosciences).

Nitric Oxide Determination. A total of 50 μL of sulfanilamide solution (1% weight/vol of sulfanilamide in 5% weight/vol phosphoric acid) were added to 50 μL of sample. After a 10-min incubation in the dark, 50 μL of 0.1% weight/vol *N*-(naphthyl) ethyl-enediamidedihydrochloride was also added, and an incubation was performed for 10 min in the dark. Absorbance at 550 nm was measured, and the amount of nitrite was determined using a NaNO2 standard curve.

Isolation of Total RNA and Real-Time RT-PCR. Total cellular RNA was isolated with TRIzol Reagent (Invitrogen). cDNA was prepared by reverse transcription (Thermoscript RT; Invitrogen) and amplified by PCR. Reactions were performed in triplicate. The oligonucleotides used are the following: b-actin—5′-TCAGAAGAACTCCTATGTGG-3′/5′-TCTCTTTGATGTCACGCACG-3′; iNOS—5′-TCCTGGAGGAAGTGGGCCGAAG-3′/5′-CCTCCACGGGCCCGGTACTC-3′; Arg1—5′-CAGAAGAATGGAAGAGTCAG-3′/5′-CAGATATGCAGGGAGTCACC-3′; Ym1—5′-GCAGAAGCTCTCCAGAAGCAATCCTG-3′/5′-ATTGGCCTGTCCTTAGCCCAACTG-3′; and Fizz1—5′-GCTGATGGTCCCAGTGAATAC-3′/5′-CCAGTAGCAGTCATCCCAGC-3′.

Amplification was performed in a 7500 Fast Real-Time PCR System (Applied Biosystems). The amplification efficiencies were the same as the one of b-actin as indicated by the standard curves of amplification, allowing us to use the following formula: fold difference = $2^{-(DCtA - DCtB)}$, where Ct is the cycle threshold. Reactions were performed in triplicate for statistical evaluation.

Detection of miR-155 Expression. Total RNA was isolated using the TRIzol reagent (Invitrogen). The expression of miR-155 was evaluated with the Taq Man microRNA Assay Kit (Applied Biosystems) using specific qRT Primer Sets, in accordance with the manufacturer's instructions (Applied Biosystems). Expression of RNU48 was used as an internal control.

Arginase Activity Determination. Arginase activity was assessed indirectly by measuring the concentration of urea generated by the arginase-dependent hydrolysis of L-arginine. Cells were lyzed with 100 μL of 0.1% Triton X-100. After 30 min on a shaker, 100 μL of 25 mM Tris·HCl was added. Into 100 μL of this lysate, 10 μL of 10 mM MnCl2 was added, and the enzyme was activated by heating for 10 min at 55 °C. Arginine hydrolysis was conducted by incubating the lysates with 100 μL of 0.5 M L-arginine (pH 9.7) at 37 °C for 60 min. The reaction was stopped with 800 μL of H2SO4 (96%)/H3PO4 (85%)/H_2O (1/3/7, vol/vol/vol). The urea concentration was measured at 550 nm after addition of 40 μL of α-isonitrosopropiophenone (Sigma-Aldrich) (dissolved in 100% ethanol), followed by heating at 100 °C for 30 min. One unit of enzyme activity is defined as the amount of enzyme that catalyzes the formation of 1 μmol·urea/min.

DSS-Induced Colitis Model. Age-matched mice received 3.5% weight/vol DSS (36–50 kDa, MP Biomedicals) in the drinking water for 5 d followed by 3 d of autoclaved water administration. The animal weight was recorded daily. Mice were euthanized at day 9, and samples were collected.

Chemokine/Cytokine Determination in Colon Extracts. Tissues were removed, washed with PBS, and cut in small pieces. For cytokine and chemokine measurement, 0.1 g of tissue was homogenized in 500 μL of 50 mM Tris·HCl buffer, pH 7.4, containing protease inhibitor mixture tablets (Roche). Samples were centrifuged at 30,000 × *g* for 20 min and assayed using a bead-based ELISA (Lincoplex, Millipore) following the manufacturer's indications.

Caecal Ligation and Puncture Model of Polymycrobial Sepsis. Caecal ligation and puncture (CLP) was performed in C57BL/6J mice as previously described (2). Briefly, mice were anesthetized with ketamine (100 mg/kg) and xylazine (8 mg/kg), and a 1-cm midline incision was made to expose the cecum. The distal 0.5-cm portion of the cecum was ligated with a 4–0 silk ligature suture without interrupting intestinal continuity. The cecum was punctured twice through and through with a 21-gauge needle and squeezed softly. The cecum was returned to the abdomen, and the incision was closed in layers with a 2–0 silk suture. After the procedure, the animals were fluid-resuscitated with sterile saline (1 mL) injected s.c. Sham controls were subjected to the same procedures as CLP without ligation and puncture of the cecum. Sera were collected from the tail vein 6 h following CLP. Bacterial burden was estimated in peritoneal lavage with 5 mL of sterile PBS at 24 h or at time of death as previously described (3). Neutrophil infiltration was estimated in the peritoneal lavage. Briefly, cells contained in 100 μL of peritoneal lavage fluid were placed on microscopic slides using cyto-spin method and stained with Giemsa stain. Neutrophils were counted under the microscope. Aspartic transaminase (AST) was determined photometrically in an Olympus/Beckman AU5400 analyzer.

T-Cell Stimulation. Spleen cells were isolated from WT, $Akt1^{-/-}$, and $Akt2^{-/-}$ mice by dislodging the tissue into 5 mL of RPMI and filtration through a 70-μm cell strainer. Red blood cells were lysed in 0.165 M NH4Cl. Splenocytes free of red blood cells were plated in a 96-well plate at a concentration of 10^6cells/mL and stimulated with concanavalin A (ConA) at 5 mg/mL (Sigma) or

plate-bound anti-CD3 (10 mg/mL) and anti-CD28 (100 mg/mL) (BD Biosciences) for 24 h as previously described (4). Cells were stained with labeled anti-CD4, anti-CD8, and anti-CD69 (all from eBioscience) and visualized by flow cytometry (FACSCalibur, BD Biosciences).

Histology and Histopathological Score. Tissues were washed thoroughly in PBS, fixed in 4% (wt/vol) formalin and embedded in paraffin. Sections of 5 μM were stained with hematoxylin and eosin (H&E) using standard procedures. Disease severity was measured on the basis of a histopathological score. Colon sections were scored 0–4: 0, normal tissues; 1, mild inflammation in the mucosa with some infiltrating mononuclear cells; 2, increased level of inflammation in the mucosa with more infiltrating cells, damaged crypt glands and epithelium, mucin depletion from goblet cells; 3, extensive infiltrating cells in the mucosa and submucosa area, crypt abscesses present within creased mucin depletion, and epithelial cell disruption; and 4, massive infiltrating cells in the tissue, complete loss of crypt. Sections were analyzed by light microscopy at 200× magnification, with the scorer blind to the experimental group. Three fields from different sections of each sample of colon tissue were examined for each mouse.

Lung, liver, and heart tissues were isolated from 42-wk-old WT and $Akt2^{-/-}$ mice, stained with hematoxylin and eosin and visualized at 200× magnification.

Immunoblot Analysis. For the detection, Akt1, Akt2 (Cell Signaling), Arg1 (BD Biosciences), Ym1 (StemCell Technologies), C/EBPβ (Santa Cruz), and anti-total STAT6 antibodies (Cell Signaling) were used. Blots were stripped in buffer containing 62.5 mM Tris·HCl (pH 6.7), 2% (wt/vol) SDS, 100 mM β-mercaptoethanol and stained with anti–phospho-STAT6 Tyr641 (Abcam) or with anti-phosphoAkt (Ser473). Protein loading was determined with a monoclonal tubulin antibody (Sigma) or a monoclonal actin antibody (Millipore). Proteins were visualized with the ECL Western blotting kit (ECL; Amersham Biosciences), and blots were exposed to Kodak X-Omat AR films. National Institutes of Health image software (ImageJ) was used to quantify the intensity of each band.

Total Lung Capacity. To evaluate the development of pulmonary fibrosis, a pressure–volume curve of the respiratory system was obtained by slow lung inflation to peak inspiratory pressure (PIP) of 25 cm H_2O as previously described (5). As an indicator of lung compliance, we used the total lung capacity, defined as the volume of air inflated at PIP of 25 cm H_2O, expressed as microliters.

1. Iliopoulos D, et al. (2009) MicroRNAs differentially regulated by Akt isoforms control EMT and stem cell renewal in cancer cells. *Sci Signal* 2:ra62.
2. Ness TL, Hogaboam CM, Strieter RM, Kunkel SL (2003) Immunomodulatory role of CXCR2 during experimental septic peritonitis. *J Immunol* 171:3775–3784.
3. Leelahavanichkul A, et al. (2012) Class B scavenger receptor types I and II and CD36 targeting improves sepsis survival and acute outcomes in mice. *J Immunol* 188: 2749–2758.
4. Tsatsanis C, et al. (2008) Tpl2 and ERK transduce antiproliferative T cell receptor signals and inhibit transformation of chronically stimulated T cells. *Proc Natl Acad Sci USA* 105: 2987–2992.
5. Vaporidi K, Francis RC, Bloch KD, Zapol WM (2010) Nitric oxide synthase 3 contributes to ventilator-induced lung injury. *Am J Physiol Lung Cell Mol Physiol* 299:L150–L159.

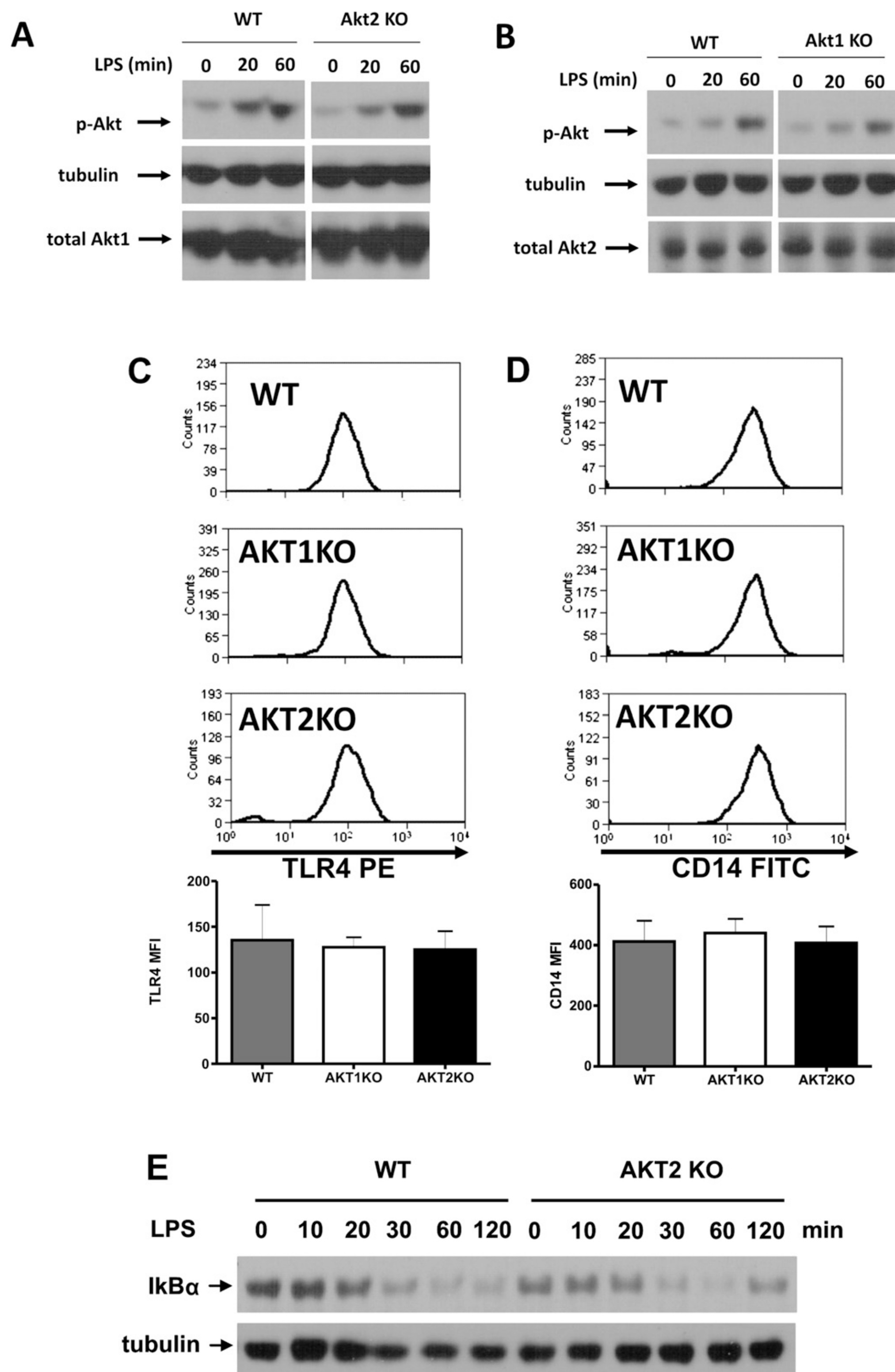

Fig. S1. Ablation of Akt1 or Akt2 does not affect LPS-induced Akt phosphorylation, does not promote compensatory changes in the expression of the other isoform, and does not affect TLR4/CD14 expression or NFkB activation. (*A* and *B*) Peritoneal macrophages from WT, Akt2$^{-/-}$ (*A*), or WT and Akt1$^{-/-}$ (*B*) mice were stimulated with LPS. Expression of phospho-Akt (Ser473) was analyzed by Western blot in the lysates. Expression levels of Akt1 and Akt2 were analyzed in the same samples. Results are representative of three independent experiments. (*C* and *D*) Thioglycollate-elicited peritoneal macrophages were stained for cell surface TLR4 and CD14 expression, and cells were visualized by flow cytometry (n = 4/group). Results are expressed as mean ± SEM. (*E*) WT and Akt2$^{-/-}$ thioglycollate-elicited peritoneal macrophages were stimulated with LPS (100 ng/mL), and IkBα expression was detected by Western blot. Results are representative of three independent experiments.

Fig. S2. Alveolar macrophages from $Akt2^{-/-}$ mice express elevated levels of Arg1. Alveolar macrophages were isolated as described in *Materials and Methods*, and expression of Arg1 on these cells was analyzed by real-time RT-PCR. Results are expressed as mean ± SEM of three independent experiments. $^{*}P < 0.05$.

Fig. S3. Deletion of Akt2 does not affect IL-4, adiponectin, or leptin levels in the serum. (*A*) Serum IL-4 was measured using an in vivo-capture method ($n = 5$/group). (*B*) Adiponectin and (*C*) leptin serum levels were evaluated by ELISA in samples obtained from WT ($n = 4$) and $Akt2^{-/-}$ ($n = 5$) mice. Results expressed as the mean ± SEM.

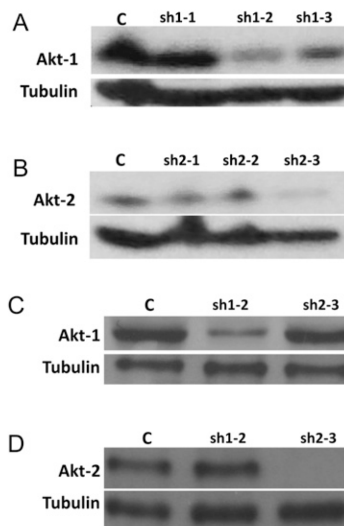

Fig. S4. Silencing of Akt1 and Akt2 in Raw264.7 cells. (*A* and *B*) Raw264.7 cells were transduced with lentiviruses expressing empty vector, shAkt1, or shAkt2. The suppression of the expression of Akt1 (*A*) and Akt2 (*B*) isoforms, respectively, was evaluated by Western blot. The most efficient shAkt1 (sh1-2) and shAkt2 (sh2-3) were used in further experiments. (*C* and *D*) Silencing of Akt1 or Akt2 with sh1-2 or sh2-3, respectively, did not affect the expression of the other isoform. Results are representative of three independent experiments.

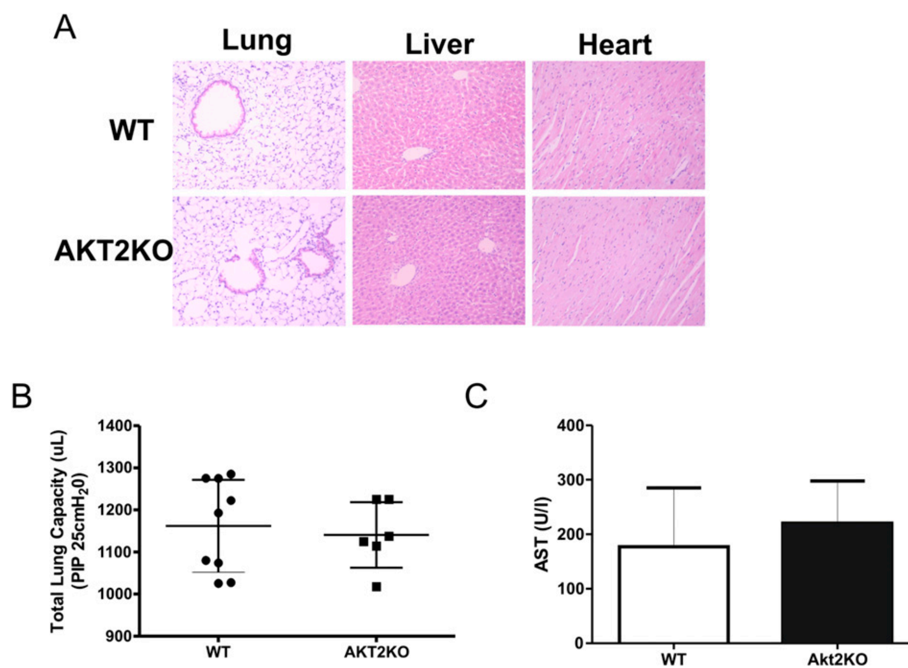

Fig. S5. Ablation of Akt2 does not result in fibrosis in the lung, heart, or liver. (*A*) Tissue samples from 42-wk-old WT ($n = 3$) and Akt2$^{-/-}$ ($n = 4$) mice were formalin-fixed, paraffin-embedded, and stained with hematoxylin and eosin and visualized at ×200 magnification. No differences were observed between WT and Akt2$^{-/-}$ tissues. Normal architecture was preserved in all tissue samples, and microscopical evidence of inflammation, fibrosis, or vasculitis was not present. No alveolar wall thickening or interstitial inflammatory infiltrates were observed in the lungs. The livers showed no portal tract distention, cholestasis, or presence of inflammation, and the interlobular bile ducts were preserved with no involutional changes. The heart tissues displayed neither signs of fibrosis nor inflammatory infiltrates. (*B*) Measuring the total lung capacity as an index of lung compliance that is reduced in fibrosis revealed no differences between WT ($n = 9$) and Akt2$^{-/-}$ ($n = 6$) mice of the same age. (*C*) Serum AST, as a measure of liver or muscle damage, did not differ between the two strains ($n = 4$/strain). Results are shown as mean ± SEM.

Fig. S6. Ablation of Akt1 or Akt2 does not alter CD69 induction on the surface of activated T cells. Splenocytes from WT ($n = 4$), $Akt1^{-/-}$ ($n = 4$), or $Akt2^{-/-}$ ($n = 4$) mice were stimulated with ConA or anti-CD3/anti-CD28 for 24 h. CD69 expression was measured on the surface of (*A*) CD4+ or (*B*) CD8+ T cells. Results are shown as mean ± SEM.